Pharmaceutical Sciences. 2025;31(4):464-479
doi:10.34172/PS.025.42131
https://ps.tbzmed.ac.ir/

Research Article

Development and Characterization of Standardized *Mesua ferrea* Linn. Extract-Loaded Phytosome Gel for Atopic Dermatitis in BALB/c Female Mice

Jugal Sutradhar[1], Debadatta Mohapatra[2], Nirupam Das[3], Alakh Niranjan Sahu[2], Bapi Ray Sarkar[1*]

[1]Department of Pharmaceutical Technology, University of North Bengal, Raja Rammohunpur, Darjeeling, West Bengal-734013, India
[2]Phytomedicine Research Laboratory, Department of Pharmaceutical Engineering & Technology, IIT (BHU), Varanasi, 221005, Uttar Pradesh, India
[3]Department of Pharmaceutical Sciences, Assam University, Silchar-788 011, India

ARTICLE INFO

Article History:
Received: January 10, 2025
Revised: July 15, 2025
Accepted: July 19, 2025
ePublished: October 11, 2025

Keywords:
Mesua ferrea Linn., Phytosome, Phytosome gel, Atopic dermatitis, DNCB-induced mice model

Abstract

Background: Atopic dermatitis (AD) is a chronic inflammatory skin disorder characterized by itching, scarring, dryness, swelling, and impaired skin barrier function. Multiconstituents-based novel vesicular phytoformulations are gaining significant attention due to their natural bioactives, excellent safety profile, and improved therapeutic activities compared to unformulated herbal drugs and conventional formulations. The study aimed to evaluate the potential of topical phytosome gel with a standardized n-hexane extract of the flowering buds of *Mesua ferrea* Linn. (SMf) for AD.

Methods: The SMf-loaded phytosome was formulated using various proportions of soya lecithin and cholesterol. It was characterized for zeta potential, vesicle size, polydispersity index (PDI), percentage of loading capacity, entrapment efficiency, and morphology by high-resolution transmission electron microscopy (HR-TEM). Subsequently, SMf-loaded phytosome was converted into gel and accessed for the organoleptic properties, pH, viscosity, spreadability, homogeneity, extrudability, syneresis, drug content, stability, ex-vivo skin permeability, drug-excipient compatibility, and therapeutic activity against AD in 1-chloro-2,4-dinitrobenzene (DNCB)-induced BALB/c female mice.

Results: The optimized phytosome formulation demonstrated the highest entrapment efficiency, drug loading, highest yield (%), low vesicle size, high zeta potential, and lowest PDI value. The phytosome gel (G-1.0) showed improved pharmaceutical properties compared to the extract-loaded plain gel formulations. The attenuated total reflectance-Fourier transform infrared spectroscopy (ATR-FTIR) study showed excellent drug-excipient compatibility. The G-1.0 gel demonstrated excellent pharmaceutical outcomes with significantly improved ex-vivo skin permeability, steady-state flux, permeability coefficient, and enhancement ratio compared to extract-loaded plain gel. Additionally, the G-1.0 gel was found non-irritant when applied topically in BALB/c female mice. The G-1.0 showed significantly higher therapeutic activity against AD in DNCB-induced BALB/c female mice than the extract-loaded plain gel.

Conclusion: The overall outcome reflected the ability of SMf-loaded phytosome gel to be a novel nanovesicular topical drug delivery system for the possible treatment of AD. However, further clinical studies are necessary to investigate the fate of the novel formulation for an effective AD treatment.

Introduction

Atopic dermatitis (AD) is the most critical chronic inflammatory skin disease, which causes scarring, rough skin, debris, itching, and swelling. Furthermore, physical symptoms, including mood disorders, behavioral problems, and an enhanced risk of depression, are associated with AD. Globally, AD often escalates in developing nations and can manifest at any stage of life, typically emerging during both childhood and adulthood. The reasons for AD are complex and multifactorial, and this chronic inflammatory skin disease affects both adults (2-10% approx.) and children (15-30% approx.).[1-3] According to the Global Burden of Disease (GBD) 2021, approximately 129 million individuals affected from AD, making it the skin disease with the highest burden.[4]

The ability of $CD4^+$ T helper lymphocyte cells to produce type-2 cytokines is quintessential in the underlying pathophysiology of AD. In particular, interleukin 17

***Corresponding Author:** Bapi Ray Sarkar, Email: brspublication@gmail.com

and 22 primarily exacerbate skin barrier disruption, allergy, and chronic inflammation.[5] AD treatment is mainly related to suppressing inflammation, decreasing itching, and resetting the skin barrier. This is achieved through both non-pharmacological and pharmacological approaches, primarily involving moisturizers and emollients that enhance the skin's barrier function and hydration.[6] While topical corticosteroids and emollients are commonly used, and their before long-term use can lead to adverse effects and inadequate symptom control.[7]

To address these limitations, there is a growing interest in herbal medicines due to their broad therapeutic potential and lower toxicity profiles. Since medieval times, herbal drugs have been utilized to treat various illnesses under local and regional healing due to their lower toxicity and being more environmentally friendly. In Southeast Asia and India, herbal products are widely accepted as part of traditional therapy, while they are considered supplementary and alternative therapies in other regions. In addition, they are regarded as nutraceuticals or dietary supplements practically everywhere.[8]

One of the large evergreen tropical trees, *Mesua ferrea* Linn. (Family: Calophyllaceae), is found across the tropical nations, including India, China, New Guinea, Burma, Thailand, the eastern Himalayan region, South Konkan, and North Canara. This medicinal plant, particularly the flowering buds, elicits anti-inflammatory, antioxidant, immune-modulatory, anti-spasmodic, anti-ulcer, hepatoprotective, analgesic, anti-arthritic, anti-microbial, anti-venom, CNS depressing, and anticancer properties.[9,10]

Despite the broad utility of herbal medicaments, considerable limitations exist in the traditional herbal drug delivery system. The larger molecular size, chemical complexity, and poor lipid solubility make them inefficient for various therapeutic uses.[11] Developing an effective novel drug delivery system (NDDS) has gained increasing attention recently. Suitable novel carriers could deliver the drug with controlled release during treatment, target the drug to the desired site of action, and ultimately produce the required therapeutic effect.[12] Several nanocarrier systems have been investigated for treating AD because they offer enhanced skin penetration and retention. These systems can load hydrophobic and hydrophilic compounds, have better safety profiles, and allow for lower doses with fewer adverse effects. Various properties, such as the nanocarrier's size, shape, and type of vehicle, can influence its ability to penetrate the stratum corneum during topical administration. [6] Phytosome is one of the NDDS of plant extracts developed by an Italian company, Indena, for multiple therapeutic uses through various routes, including topical applications.[11,13] It offers enhanced skin penetration and improved therapeutic outcomes owing to their nanostructure.[14] Further, the phospholipid of phytosome has low inherent toxicity, is non-immunogenic, biocompatible, and biodegradable.[15] Several vesicular drug delivery systems, including phytosome, ethosome, liposome, niosome, and transfersome, have been established for the loading of phytoconstituents (curcumin, lawsone, apigenin, capsaicin, paeonol) and standardized extracts (*Carum carvi*, *Terminalia chebula*) for various therapeutic purposes. These vesicular formulations represented superior therapeutic activity to plain phytoconstituents and standardized extracts by increasing solubility, permeability, absorption, and bioavailability. These vesicles are also widely exploited for topical and transdermal drug delivery with improved therapeutic efficacy.[16-18]

Among the various vesicular nanoformulations, phytosomes are recognized as a promising option for delivering herbal drugs with enhanced therapeutic efficacy. The phytosomes are composed of phospholipids and plant extract, where the phytoconstituents are complexed with phospholipid. In contrast, niosomes are composed of non-ionic surfactants, ethosomes comprise phospholipid and ethanol, transferosomes comprise phospholipid and edge activators/surfactants, and liposomes are prepared from phospholipid and cholesterol, which contain herbal drugs in their core or phospholipid bilayer. Various plant extracts (milk thistle, green tea, Ginkgo biloba, grape seed, ginseng, and hawthorn) in phytosome form have demonstrated more therapeutic efficacy compared to liposomes.[14,19] Phytosomes can penetrate skin barriers, making them efficient carriers for topical delivery of herbal drugs. By improving the bioavailability and absorption of compounds, they have broadened their clinical uses. In skincare formulations, phytosomes demonstrate greater efficacy compared to liposomes.[20,21]

Recent research reported that olive oil with a phytosomal nanocarrier of quercetin enhances skin permeability. The phytosomal nanocarrier was prepared by a solvent evaporation/anti-solvent precipitation technique and optimized using a Box-Behnken design. The formulation showed significantly higher skin permeation of quercetin compared to an olive-oil/surfactant-free formulation and the control.[22] In another study, a phytosomal gel of aloe vera extract was studied for topical drug delivery. A 2^2-factorial design was used to develop and statistically optimize the formulation concerning vesicular size and entrapment efficiency. The optimized phytosome was loaded into carbopol 934 to develop a phytosomal gel. The phytosomal gel showed significantly higher permeation and flux profile compared to the conventional aloe vera extract gel.[8] This study aimed to develop and evaluate a phytosome gel of standardized n-hexane extract of *Mesua ferrea* Linn. flowering buds for enhanced topical delivery against AD. The phytosome was formulated by the thin-film hydration method using soya phospholipid and cholesterol. The optimized phytosome demonstrated high loading capacity (% LC), entrapment efficiency (% EE), zeta potential (ZP), a small average vesicle size (Z_{avg}), and a low polydispersity index (PDI). This optimized phytosome was then incorporated into a gel and evaluated

for various properties, including organoleptic properties, homogeneity, viscosity, pH, extrudability, spreadability, syneresis, drug content, ex-vivo skin permeability, drug-excipient compatibility, stability study and therapeutic activity against AD in 1-chloro-2,4-dinitrobenzene (DNCB)-induced BALB/c female mice.

Materials and Methods

Materials

Flowering buds of *Mesua ferrea* Linn. were collected from West Bengal, India. Standard β-sitosterol (MP: 136-140 °C, MW: 414,71g/mol) was procured from Sigma-Aldrich (MO, USA). The soya lecithin (30%), cholesterol extra pure AR (99%), DNCB (99%), and carbopol 934 extra pure were obtained from Sisco Research Laboratories Pvt. Ltd. (Mumbai, India). Analytical-grade solvents were employed in the experiments without subsequent purification or distillation.

Methods

Preliminary studies of flowering buds of Mesua ferrea Linn.

The flowering buds of the medicinal plant *Mesua ferrea* Linn were collected from the University of North Bengal in India, and the plant was authenticated at Griffin's Herbarium (Voucher specimen no. Calophylla. 2021/1) by Prof. N.K. Dubey, at Centre of Advanced Study in Botany, Institute of Science, Banaras Hindu University, Varanasi 221005. Various quality measurements were conducted on the powder sample of *Mesua ferrea* Linn. flowering buds, including bulk density, tapped density, Hausner ratio, angle of repose, and Carr's index. For physicochemical evaluations, the foaming index, ash values, swelling index, and loss on drying were assessed. Extracts were obtained through the maceration method, utilizing solvents ranging from low-polar to high-polar. Additionally, primary phytochemical screening was performed, which included tests for glycosides, flavonoids, alkaloids, tannins, steroids, and carbohydrates.[23]

A solvent system ratio (6:2:0.1) v/v of toluene, ethyl acetate, and acetic acid was developed for high performance thin layer chromatography (HPTLC) analysis at 254 nm, using the reference β-sitosterol having an R_f value of 0.83. A validated HPTLC method enabled the quantitative estimation of β-sitosterol. The standard curve was generated using various concentrations of β-sitosterol found in SMf. The analytical process included supporting studies on the limit of quantification, specificity, limit of detection, accuracy, recovery, and precision, all of which validated the methods used. Additionally, a well diffusion method was employed for antimicrobial investigation, and the minimum inhibitory concentration was subsequently determined.[24]

Formulation and development of phytosome

SMf-loaded phytosomes were prepared using the thin film hydration method. The required amount of SMf, soya lecithin, and cholesterol at various ratios (1:1:0.25; 1:2:0.25; 1:3:0.25) was mixed with 30 mL of chloroform in a 100 mL round bottom flask and sonicated for 25 minutes to achieve molecular interaction with formulation components and accomplish solubilization. The organic solvent was removed through a rotary vacuum evaporator at 60 °C with 75 rpm until a uniform thin film was formed on the flask walls and hydrated with phosphate-buffered saline (pH 7.4) overnight to produce phytosome vesicles. The phytosome was sonicated by a probe sonicator (Hielscher ultrasound technology, Germany) at 60% amplitude with one cycle (at an interval of 60 seconds) to reduce the vesicular size. Then, the phytosome formulations (P1, P2, and P3) were stored in glass vials and protected from light. The placebo phytosome (P0) without SMf was formulated for comparison purposes.

Evaluation of phytosome

Zeta potential, hydrodynamic vesicle size, and polydispersity index

The dynamic light scattering (DLS) instrument (Malvern Zetasizer Pro, UK) was used to measure the PDI, Z_{avg}, and ZP at 25°C. The Z_{avg} and PDI were measured using a polystyrene cuvette, where the zeta potential was measured using a universal dip cell with water as a dispersion medium.

Yield, entrapment efficiency, and loading capacity

The percentage yield of the phyto-phospholipid complex (phytosome) was calculated by equation 1, and the percentage of LC and EE with respect to β-sitosterol was measured by the validated HPTLC method. Centrifugation was used to separate the free drug from the supernatant at 20 000 rpm at 4 °C for 60 min using a high-speed refrigerated centrifuge (Hermle, Z 32 HK, Sayreville, New Jersey, USA). The quantity of β-sitosterol in the supernatant was calculated using HPTLC at 254 nm. Equations 2 and 3 were used to determine the percentage of EE and LC, respectively.

$$\%\ \text{Yield} = \frac{\text{Amount of phyto} - \text{phospholipid complex obtained}}{\text{Total amount of SMf and excipients taken}} \times 100 \quad (1)$$

$$\%\ \text{EE} = \frac{\text{Amount of encapsulated } \beta - \text{sitosterol}}{\text{Total amount of } \beta - \text{sitosterol in the used SMf}} \times 100 \quad (2)$$

$$\%\ \text{LC} = \frac{\text{Amount of encapsulated phytoconstituent}}{\text{Total amount of excipients used}} \times 100 \quad (3)$$

High-resolution transmission electron microscopy (HR-TEM)

The vesicular morphology of optimized phytosome (P3) was examined by the HR-TEM (TECNAI G2 F20 TWIN, FEI, USA) with an HAADF detector. The P3 was diluted with type-1 water, sonicated for 5 min, and 15 µL of the sample was dropped onto a carbon-coated copper grid (Ted Pella, mesh size: 300, diameter: 3.05 mm), then dried overnight and subjected to the instrument for morphology analysis. The photomicrograph was analyzed using ImageJ software (version 1.53e) to measure vesicle size and distribution.

Formulation of phytosome-loaded nanovesicular gel

P3 (containing 300 mg of SMf) was loaded into carbopol 934 based gel of three distinct concentrations (0.5 % w/v, 1.0% w/v, and 1.5% w/v) and a few (2 drops) of triethanolamine (TEA) were added to maintain the pH and continuously stirred to produce a uniform gel. SMf-loaded plain gel (G-SMf) and placebo gel (G-placebo: with placebo phytosome) containing 1% w/v of carbopol 934 were prepared for comparison. The composition of various phytosome gels is represented in Table 1. The formulations were placed in screw-capped glass containers for further evaluation.

Characterization of phytosome-loaded gel

Organoleptic properties, pH, homogeneity, and viscosity

The appearance and color were examined through the naked eye.[25] A calibrated digital pH meter (Eutech Instrument, P700) was used to measure the pH of each gel at room temperature. The appearance, presence of any aggregates, and homogeneity were assessed through visual examination. The viscosity of each gel formulation was measured by the Brookfield viscometer (LVT Model) with spindle No. 64 at 12 rpm at 25 °C.[26]

Extrudability and spreadability

For the extrudability study, the weight in grams required to extrude a 0.5 cm ribbon of gel in 10 seconds from a collapsible tube was measured. To assess the spreading ability of the gel, 500 mg of gel was placed inside a 1 cm diameter circle previously marked on a 3 mm thick glass plate. A second glass plate was then placed on top, along with a 500 g weight, for five minutes. The spreadability of the gel was evaluated by measuring a minimum of three diameters of the spread area for each formulation.[26,27]

Syneresis

This test involved placing gels in a cylindrical centrifuge tube and determining the initial weight (M1). The tubes were centrifuged for 15 minutes at 5000 rpm, and the released (free) water was thrown away and re-weighed (M2). Equation 4 was used to determine the syneresis.[28]

$$\% \text{ Syneresis} = \frac{(M1 - M2)}{M1} \times 100 \quad (4)$$

Drug content determination

The drug content of SMf was determined through the validated HPTLC method. Each gel (300 mg) was diluted with 5 mL methanol, sonicated, vortexed, and centrifuged at 5000 rpm for 15 minutes. Finally, the content of β-sitosterol was determined *via* validated HPTLC.[25]

Compatibility study through attenuated total reflectance-Fourier transform infrared spectroscopy (ATR-FTIR)

FTIR spectroscopic analysis was used to study drug-excipient compatibility. ATR-FTIR spectroscopy (Bruker Alpha II, Bruker Optics, Ettlingen, Germany) records the vibrational spectra of phytosomes, individual ingredients, and their physical mixture. Before the ATR-FTIR analysis, the gels were freeze-dried for 12 hours to prevent the dominant broad peak of water.

Ex-vivo skin permeability study

The ex-vivo skin permeability studies of phytosome gel were carried out as per the previous protocol.[29,30] In detail, the vertical Franz diffusion cell (50 mL and diameter 2.5 cm) was used for the ex-vivo permeability tests. The goatskin (thickness 0.4 mm) was procured from the slaughterhouse. The sticky, fatty material of the skin was eliminated using a cotton swab and isopropyl alcohol. The skin was preserved at -20°C in aluminium foil until required. The goatskin was attached between the donor and receptor compartments. Phosphate buffer (pH 7.4) with Tween 80 (0.5%) was used as a diffusion medium. To prevent microbial development, sodium azide (0.0025% w/v) was added to the medium. The medium was stirred by magnetic stirrers at 150 rpm and maintained at 37 ± 0.2 °C. One gram of extract-loaded plain gel (G-plain) and the equivalent amount of phytosome gel (G-1.0) were applied to the goat skin. Intermittently, 1 mL of the sample was taken out and replaced with an equal amount of diffusion media at 0, 0.25, 0.5, 1, 1.5, 2, 3, 4, 6, 8, 10, 14,18, and 24 h to maintain the sink condition. Then the samples are diluted with methanol, centrifuged, and filtered with a 0.22 µm membrane filter. The supernatant was used to quantify the drug using the validated HPTLC method. The cumulative amount of β-sitosterol permeation over a unit area at a predetermined time is calculated by the following equation 5.[31]

Table 1. Composition of SMf loaded-phytosome gel, SMf loaded-plain gel, and placebo gel.

Gel Formulation Code	300 mg SMf loaded optimized P3 (mL)	Plain Phytosome (mL)	Carbopol-934 (mg)	Triethanolamine drops	SMf (mg)	Distilled Water (mL)
G-0.5	20	-	125	2	-	5
G-1.0	20	-	250	2	-	5
G-1.5	20	-	375	2	-	5
G-SMf	-	-	250	2	300	25
G-placebo	-	20	250	2	-	5

Note. The (-) sign indicates the absence of ingredients, G-0.5 (0.5 % w/v phytosome gel), G-1.0 (1.0 % w/v phytosome gel), and G-1.5 (1.5% w/v phytosome gel), G-SMf (SMf loaded 1.0% w/v plain gel), and G-placebo (Placebo phytosome-loaded 1.0% w/v gel)

$$\text{Cumulative amount}(\text{Qi}) = \frac{c_i V + \Sigma_1^{i-1} C_{i-1} \text{X } Vi}{A} \quad (5)$$

Where [Qi] - the cumulative amount of drug, [A] - diffusional area (4.908 cm^2); [V] - the volume of the receptor medium (50 mL); [Ci] - drug concentration at a predetermined time [i] in receptor medium; [Vi] represents the volume after each sampling time; [$\Sigma_1^{i-1} C_{i-1}$] a total of the previously measured concentrations. The permeability coefficient (kp) was calculated by equation 6.

$$\text{Permeability coefficient (kp)} = (dQ/dt)/ACd \quad (6)$$

Where A is the diffusion area, Cd is the drug concentration in the donor compartment, and dQ/dt is the slope from the penetration study. The slope of the linear region of the graph was divided by the surface area of the diffusion cell to determine the drug permeation rate (flux) in a steady state (Jss). The equation is (dQ/dt)/A, where A is the diffusion area, and dQ/dt slope, and the enhancement ratio (Er) was measured by equation 7.[32,33]

$$\text{Enhancement ratio} = \frac{\text{Drug permeation rate (flux) of phytosome gel}}{\text{Drug permeation rate (flux) of control gel}} \quad (7)$$

Heating–cooling cycles stability study

The heating–cooling cycles stability study was accomplished as per the reported methods by Tunit et al[34] with slight modifications. The phytosome was evaluated for physical appearance, zeta potential, vesicle size, and PDI. The optimized phytosome-loaded gel was evaluated through physical appearance and liquid loss measurement (syneresis). This study was performed with three cycles at 2 °C and 45 °C. The stability study of phytosome and phytosome gel was evaluated by calculating each value at the end of each cycle.

Animal study

Experimental animals

Seven-week-old female BALB/c mice (20 ± 2.015 g body weight) were kept in standard cages at 20 °C to 24 °C, 50 to 60% relative humidity, with a 12-hour light and dark cycle, with food and water ad libitum. The studies were carried out with the necessary approval from the Deshpande Laboratories Pvt. Ltd. (An ISO 9001:2008 Certified Drug Testing Laboratory CPCSEA), with number 1582/PO/Re/S/11/CPCSEA, Date. 31.01.2023, and by the recommendations of the CPCSEA. Further, the study was conducted in conformity with the guidelines of animal research: reporting of in vivo experiments.[35]

Acute toxicity and irritation study on skin

Acute dermal toxicity and skin irritation studies were performed according to the Organization for Economic Co-operation and Development (OECD) guideline 402.[36] The mice were housed separately to prevent other animals' ingestion of the test sample. Before topical treatment, the hair was removed from 10% of the total body surface area from the dorsal side of BALB/c mice. The SMf was slightly wet with distilled water to improve contact with the skin. The SMf was applied topically as a very thin layer at 100 and 200 mg/kg doses. The control group represents the animals administered topically with distilled water. A porous gauze dressing was used to ensure the 24h skin retention of SMf and avoid animal self-ingestion.

Animals were monitored after dosing at least once within the first 30 minutes and several times during the first 24 hours. Observations continued daily for the following 14 days, with special attention given to the initial 2 to 6 hours after the start of the exposure period. After 24 hours, the substance was removed, and the treatment site was carefully examined at 24, 48, and 72 hours for any signs of redness, dryness, irritation, swelling, inflammation, or other abnormalities.

The Draize patch test was performed to evaluate the skin irritancy property of the phytosome gel on the female BALB/c mice. The G-1.0 (equivalent to 300 mg/kg of SMf) was applied uniformly to the shaved dorsal side of four BALB/c mice and covered by a gauze dressing to avoid self-ingestion. The control group comprised mice with shaved skin but without any topical application. After 24 hours, the gel was precisely removed, and the skin surface was examined for signs of erythema and edema. The observed responses were documented as the primary irritation index (PII).[37]

Induction of atopic dermatitis and efficacy evaluation

The induction of AD was carried out as per the previous protocol with minute modifications.[38] For the induction of AD, the dorsal side of the skin and right ears of BALB/c female mice (7 weeks old, weighing 19 ± 2.015 g) were sensitized with DNCB. An electric clipper removed the hair from the dorsal side. Except for the normal control group, the remaining mice were sensitized with 200 µL and 30 µL 1% DNCB solubilized in a mixture of olive oil-acetone solution (1:3 v/v) on their back skin and right ears, respectively, for three successive days. Then, the mice were challenged with 0.5% DNCB every alternate day for 35 days.

BALB/c female mice were randomly divided into seven groups (n = 4 per group) as follows: The normal control group (without induction of AD), the disease control group (induction of AD without any treatment), the G-placebo group (without standardized extract phytosome gel), the SMf group (purely standardized plant extract), the G-SMf group (SMf-loaded plain gel), the G-1.0 group (treatment with optimized SMf-loaded phytosome gel), and the betamethasone group (standard marketed product, Betagel®). The study used a topical dose of 15.527 mg/kg of SMf and an equivalent dose of gel formulations. The treatments were continued after initial sensitization for 5 weeks on every alternate day so that the application of 0.5% DNCB and treatment would not occur on the same day.

Measurement of ear thickness, spleen weight, blood parameters, and cytokines

The ear thickness of BALB/c mice was measured using a digital caliper (Jipvi Ecommerce Pvt. Ltd., China). The spleen weight of each group of mice was measured on the day of sacrifice.[39,40] The levels of hematological parameters (WBC, neutrophils, monocytes, lymphocytes, and eosinophils) and cytokines (TNF-α, IL-4, IFN-γ) were measured following the manufacturer's instructions. For the measurements mentioned above, blood samples were obtained from the retroorbital plexus, and serum was recovered by centrifugation and stored at -20 °C for further research. ELISA kits (BioVendor-Laboratorní medicína a.s., Brno, Czech Republic) were used to measure the serum levels of TNF-α, IFN-γ, and IL-4 as per the manufacturer's instructions.[41,42]

Statistical analysis

The data for each group were analyzed using one-way ANOVA, and the statistical outcomes were presented as SD ± SEM. Tukey's comparison test was employed to assess the significance between various groups. GraphPad Prism 5 was used for the statistical analyses, and $P \leq 0.05$ was considered significant.

Results

Preliminary studies

The physicochemical investigation and the powder sample's micrometric characteristics were found to be satisfactory. According to the preliminary phytochemical analysis, all extracts have carbohydrates, steroids, and flavonoids in ethanol and ethyl acetate extract. The HPTLC study confirmed that every extract contains β-sitosterol, and validation of β-sitosterol showed linearity within 1.0-3.0 µg/spot with a regression equation of $y = 0.0033x + 0.003$, $r^2 = 0.9918$ (n = 3). The linear regression data of the calibration plot are measured and found the range (1.0-3.0µg/spot), linearity (0.9918, n = 3), limit of detection (0.40 µg/spot), limit of quantification (1.22µg/spot) at 254nm. The average recovery study of β-sitosterol is 99.98 % in concentration (50 %, 100 %, 150 % µg/Spot). The chromatogram of the extract had a peak with an R_f value ranging from 0.800 to 0.824 for the sample and is near the R_f (0.837) for the reference β-sitosterol. The extractive yield of the n-hexane extract was 2.1%, and the amount of β-sitosterol was 161mg per gram of dried SMf. The n-hexane extract of SMf showed potent anti-microbial activity against *Staphylococcus aureus* with a 0.062 mg/ml MIC value.[23,24]

Characterizations of SMf-loaded phytosome formulations and optimization

The prepared formulations (P1, P2, P3) were found to be homogeneous liquids with a slightly yellowish-white color. Table 2 shows the evaluated results of phytosome formulations, and the HR-TEM photomicrograph of P3 is shown in Figure 1a. Most of the vesicles are found to be within 20-22 nm (Figure 1b). The selected area electron diffraction (SAED) pattern (Figure 1c) showed the diffused concentric rings, representing the amorphous nature of the vesicles.

Characterization of phytosome-loaded gel

Table 3 shows the characterization outcomes of gel formulations. G-1.0 was used for further studies because it was close to the marketed formulation's viscosity, spreadability, extrudability, and syneresis.

Drug excipient compatibility

The ATR-FTIR study aimed to understand the potential molecular interactions among the components of the phytosome gel and the standardized extract. The comparative results of each formulation component and the optimized phytosome gel are represented in Figure 2a. The standardized extract exhibits distinctive peaks at 3436 cm^{-1}, corresponding to the stretching of phenolic -OH groups. Additionally, the bands observed at 2922 cm^{-1} and 2860 cm^{-1} signify the stretching vibrations of alkane C–H bonds. Notably, peaks at 1715 cm^{-1} denote the C = O stretching in ketones, while the 1660 cm^{-1} peak indicates the –C = C– stretching in alkenes. Other essential features include peaks at 1544 cm^{-1} (asymmetric stretch of N–O), 1448 cm^{-1} (C–C aromatics stretching), and 1372 cm^{-1} (C–H rocking of alkanes). The signals at 1283 cm^{-1} and 1229 cm^{-1} are attributed to the C-O stretching in esters or ethers. Additionally, the bands at 1160 cm^{-1} are linked to C–H wagging, and 1077 cm^{-1} is associated with the C-N stretching of the alkyl group.

Ex-vivo skin permeability

The skin permeability of the formulations was assessed using the Franz diffusion cell. In Figure 2b, the phytosome gel (G-1.0) demonstrated significantly higher cumulative drug permeation ($P < 0.05$) compared to the standardized extract-loaded plain gel (G-plain). The permeability coefficient (Kp) was notably higher for G-1.0 [1.90 ± 0.006

Table 2. Characterizations of the phytosome formulations

F Code	Yield (%)	Z_{avg} (nm)	PDI	ZP (mV)	EE (%)	DL (%)
P1	95.8 ± 0.10	81.33 ± 1.11	0.26 ± 0.11	38.83 ± 0.23	44.44 ± 1.23	9.55 ± 0.27
P2	94.17 ± 0.30	76.73 ± 1.35	0.47 ± 0.11	43.43 ± 0.65	51.10 ± 0.27	10.85 ± 0.79
P3	95.28 ± 0.29	72.16 ± 2.38	0.22 ± 0.08	50.36 ± 0.43	60.71 ± 0.47	6.93 ± 0.33
P0	96.08 ± 0.36	71.03 ± 0.44	0.24 ± 0.08	25.32 ± 0.64	0.00 ± 0.00	0.00 ± 0.00

F Code: Phytosome formulations code ZP: Zeta potential, Z_{avg}: Average vesicular size, PDI: Polydispersity index, DL: Drug loading.

Table 3. Characterization of various types of gel formulation.

Parameter of phytosome loaded gel	G-0.5	G-1.0	G-1.5	G-SMf	G-placebo	Control (Deloff®, Genext labs)
Organoleptic properties	White color, opaque, and no phase separation	White color, opaque, and no phase separation	White color, opaque, and no phase separation	Slight yellowish color, opaque, and no phase separation	White color, opaque, and no phase separation	Brown color, translucent, and no phase separation
pH	5.51 ± 0.06	5.49 ± 0.03	5.15 ± 0.03	5.65 ± 0.28	6.14 ± 0.12	5.34 ± 0.05
Homogeneity	Homogeneous	Homogeneous	Homogeneous	Heterogeneous	Homogeneous	Homogeneous
Texture	Smooth	Smooth	Smooth	Slight Smooth	Smooth	Smooth
Viscosity (cP)	41666 ± 882.96	74333 ± 333.72	110666 ± 667.45	78576 ± 762.23	75633 ± 454.14	73666 ± 432.21
Spreadability (cm)	7.31 ± 0.06	6.76 ± 0.10	5.9 ± 0.053	6.85 ± 0.15	6.98 ± 0.02	6.63 ± 0.07
Extrudability (g)	182.23 ± 1.04	139.76 ± 2.22	113.28 ± 1.52	120.27 ± 2.08	151.04 ± 1.52	132.21 ± 2.10
Syneresis (%)	2.01 ± 0.16	1.45 ± 0.15	1.06 ± 0.21	1.82 ± 0.78	1.62 ± 0.10	1.22 ± 0.10
Drug content (%)	97.05 ± 2.14	97.94 ± 2.23	96.39 ± 1.27	98.03 ± 2.26	0	--

Sign (0) indicate no SMf added, and (--) sign cannot perform the drug content study.

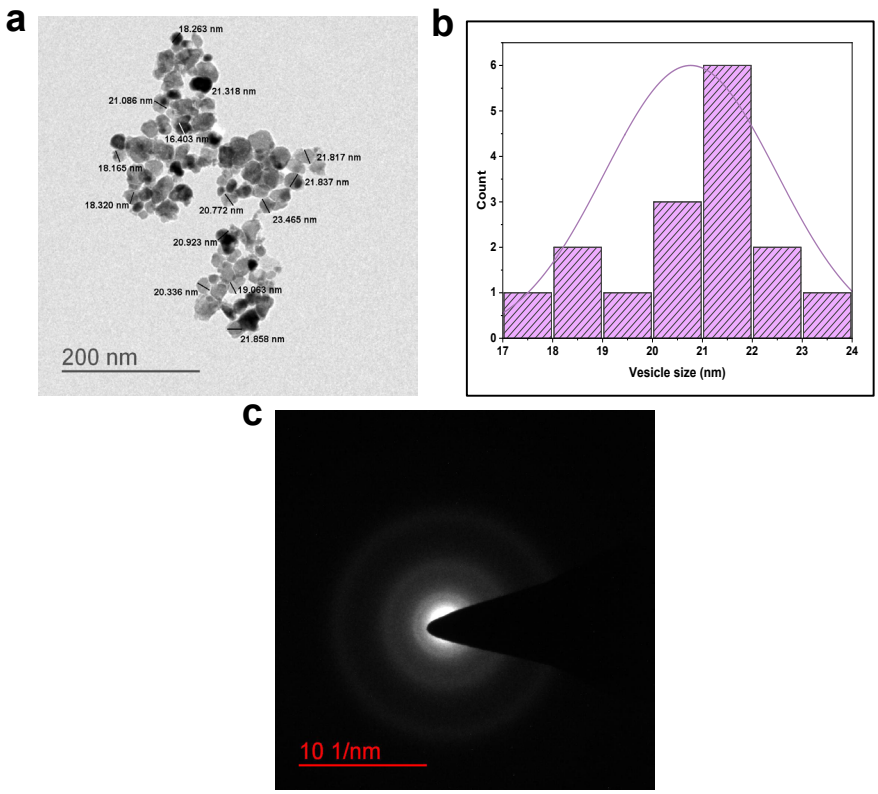

Figure 1. HR-TEM photomicrographs, size distribution, and SAED pattern of optimized phytosome **(a)** Photomicrograph of optimized phytosome formulation (P3) at 200nm scale; **(b)** Particle size distribution of phytosome vesicles; and **(c)** SAED pattern of phytosome. HR-TEM: High-resolution transmission electron microscopy, SAED: Selected area electron diffraction

$h^{-1}.cm^{-2}$] in comparison to the extract-loaded plain gel [1.45 ± 0.020 $h^{-1}.cm^{-2}$]. The steady-state flux (Jss) of the drug from G-plain and G-1.0 was 0.23 ± 0.003μg.$h^{-1}.cm^{-2}$ and 0.30 ± 0.001μg.$h^{-1}.cm^{-2}$, respectively, resulting in an enhancement ratio (Er) of 1.304.

Stability study

The heating–cooling cycles (three cycles) stability study of both the optimized formulation of phytosome with SMf, soya lecithin, and cholesterol ratio 1:3:0.25 (P3) and phytosome gel with 1.0 % w/v SMf-loaded phytosome formulations are shown in Table 4.

Acute dermal toxicity and skin irritation study

After 14 days, no animal deaths were observed at up to the highest topical dose of SMf. The results of skin irritation for SMf are shown in Table 5.

Animal study on the DNCB-induced mice model

The disease control group demonstrated a prominent increase ($P < 0.001$) in both ear thickness and spleen weight compared to the normal control group, indicating the manifestation of phenotypes associated with AD. In contrast, the G-placebo group displayed a non-significant alteration ($P > 0.05$) in spleen weight and ear thickness compared to the disease control group, indicating a

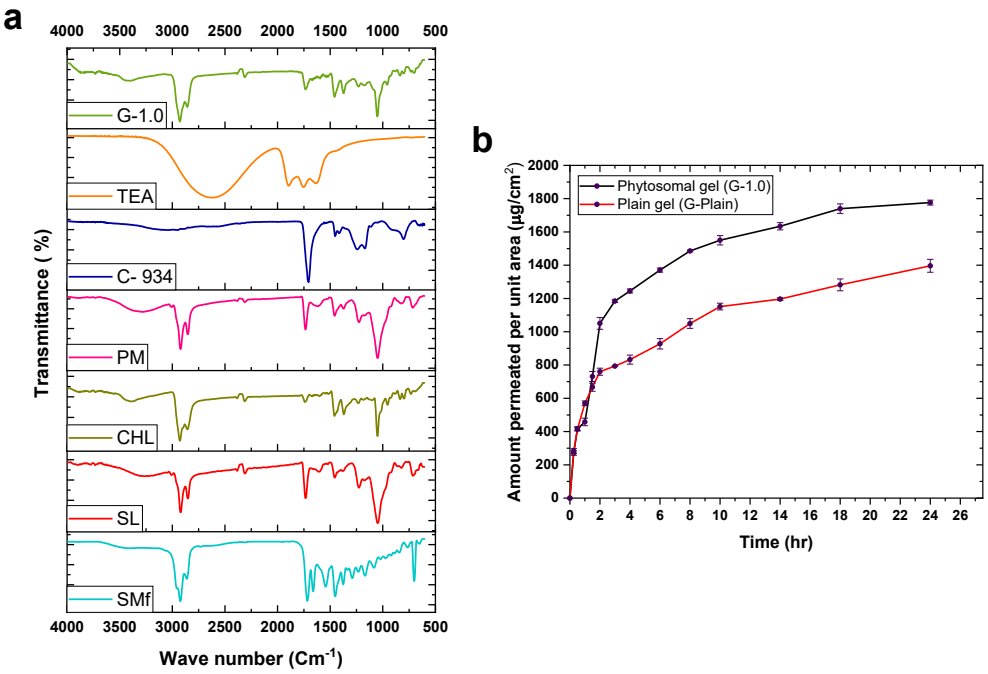

Figure 2. Drug-excipient compatibility and ex-vivo skin permeability study **(a)** ATR-FTIR study for drug-excipient compatibility analysis, and **(b)** *Ex-vivo* skin permeation study of phytosome gel (G-1.0) and SMf-loaded plain gel (G-plain). SMf (Standardized extract), SL (Soya lecithin), CHL (Cholesterol), PM (Physical mixture), C-934 (Carbopol 934), TEA (Triethanolamine), G-placebo (Placebo phytosome added to 1.0% w/v gel), and G-1.0 (Phytosome gel). ATR-FTIR: Attenuated total reflectance-Fourier transform infrared spectroscopy

Table 4. Heating–cooling cycles of SMf-loaded phytosome and SMf-loaded phytosome gels.

Stability study cycles	SMf-loaded phytosome formulations				SMf-loaded phytosome gel formulations	
	PAp	Z_{avg} (nm)	ZP (mV)	PDI	PAg	Rs (%)
Initial	White color, no precipitation	75.33 ± 1.52	49.46 ± 0.28	0.22 ± 0.08	White color, opaque, Smooth	1.45 ± 0.15
Cycle-1	White color, no precipitation	89.23 ± 1.33	48.23 ± 0.22	0.31 ± 0.02	White color, opaque, Smooth	2.16 ± 0.21
Cycle-2	White color, no precipitation	143.42 ± 2.45	45.65 ± 0.33	0.38 ± 0.08	White color, opaque, Smooth	2.67 ± 0.25
Cycle-3	Slight yellowish color, slightly precipitation	204.28 ± 3.29	30.32 ± 0.13	0.40 ± 0.09	Light brown color, opaque, no visible aggregation	3.32 ± 0.22

PAp: Physical appearance of SMf-loaded phytosome formulations, PAg: Physical appearance of SMf-loaded phytosome gel formulations, ZP: Zeta potential, Z_{avg}: Average vesicular size, PDI: Polydispersity index, Rs: Syneresis

Table 5. Skin irritation scores of treated and untreated group BALB/c mice skin.

Signs and symptoms of skin	Treated	Untreated	Treated	Untreated
	100 mg/kg 24 hours n = 4		200 mg/kg 24 hours n = 4	
Redness	*	*	*	*
Dryness	**	*	**	*
Irritation	**	*	**	*
Swelling	*	*	*	*
Inflammation	*	*	*	*
Other Signs	-	-	-	-

The stare sign (*) indicates * None, **Very Mild, redness, dryness, irritation, swelling, inflammation, and other signs (-) indicate absent of sign and symptoms.

lack of therapeutic activity from the excipients. The SMf group showed a significantly decreased level of the above parameters compared to the disease control group, reflecting the ability of the standardized extract to treat AD. The G-1.0 displayed a further significant decrease ($P < 0.001$) in the ear thickness and spleen weight compared to the G-SMf, which is due to the enhanced dermal permeation ability of SMf-loaded phytosome nanovesicles compared to the neat SMf. The marketed betamethasone dipropionate gel (Betagel®, Micro Labs Ltd.) showed a significant decrease in the levels of hematological parameters compared to the disease control group. The result of G-1.0 is well comparable with the marketed gel formulation employed (Figure 3).

Similarly, the TNF-α, IL-4, and IFN-γ levels are significantly higher ($P < 0.001$) in the case of the disease control group compared to the normal control. All the treatment groups showed a significant decrease ($P < 0.001$) in the levels of cytokines compared to the disease control group. The G-1.0 showed a significant decrease ($P < 0.05$) in the TNF-α, IL-4, and IFN-γ levels compared to the G-SMf due to the nanostructure and enhanced dermal

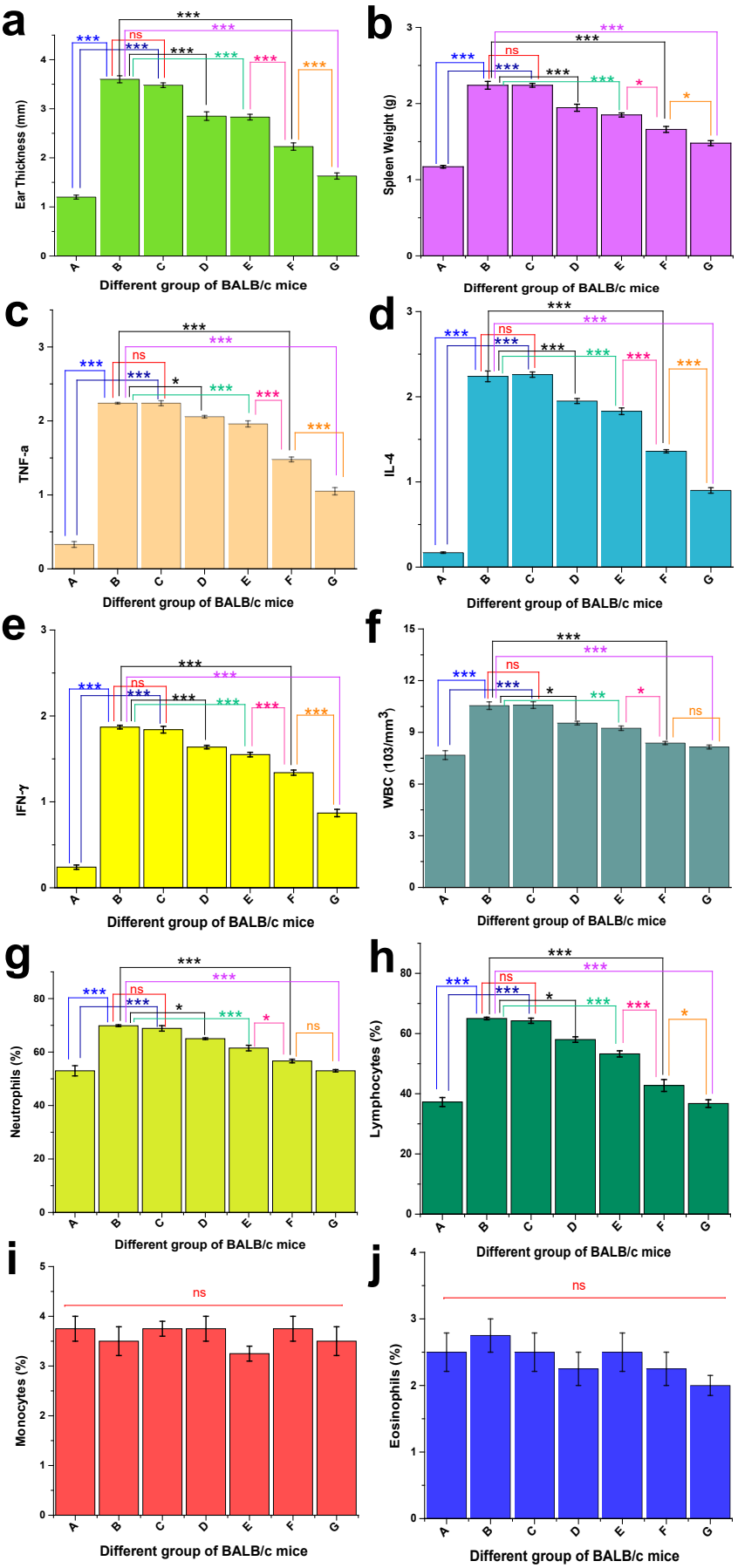

Figure 3. Results of in-vivo studies in DNCB-induced BALB/c female mice **(a)** Ear thickness, **(b)** spleen weight, **(c)** TNF-α (Tumor necrosis factor alpha), **(d)** IL-4 (Interleukin 4), **(e)** IFN-γ (Interferon-gamma), **(f)** WBC (white blood cells), **(g)** neutrophils, **(h)** lymphocytes, **(i)** monocytes, and **(j)** eosinophils where, **A.** Normal control group, **B.** Disease control group, **C**. G-placebo group, **D.** SMf group, **E.** G-SMf group, **F.** G-1.0 group, **G.** betamethasone group

permeation. The marketed gel showed a significant decrease in the levels of the evaluated parameters.

The disease control group showed a significant increase in the level of WBC ($P < 0.001$), neutrophils, and lymphocytes compared to the normal group. The G-placebo group showed a non-significant change ($P > 0.05$) in the parameters' levels compared to the disease control group, reflecting no therapeutic activity. The SMf group showed a significantly decreased level of the above parameters compared to the disease control group, reflecting the standardized extract's ability to treat AD. When comparing the neat SMf group to the G-SMf group, a decrease in the levels of the hematological parameters was observed, attributed to better retention at the topical site due to the gelling consistency. However, the G-1.0 showed a further significant decrease ($P < 0.05$) in the evaluated parameters compared to the G-SMf due to the enhanced dermal permeation ability of SMf-loaded phytosome nano vesicles compared to the neat SMf. The marketed betamethasone dipropionate showed a significant decrease in the levels of hematological parameters compared to the disease control group. Except in the case of lymphocytes, the G-1.0 showed a non-significant difference ($P > 0.05$) compared to the marketed betamethasone dipropionate, reflecting equivalent therapeutic activity. However, the levels of monocytes and eosinophils were found to be non-significant among all the evaluated groups. Following treatment with G-plain, G-placebo, SMf, G-SMf, G-1.0, marketed dexamethasone, and normal control, DNCB-induced AD-like skin condition in BALB/c mice, the use of DNCB caused substantial inflammation, as shown in Figure 3.

Discussion

The preliminary studies of *Mesua ferrea* Linn. plant powder and extracts results were in an acceptable range. According to the ICH guidelines, the developed HPTLC method was found to be validated.[43] The density of this gram-positive strain of *Staphylococcus aureus* appears to increase the severity of AD skin, with this bacterium found in 90% of cases.[44,45] The SMf shows anti-microbial activity against this Gram-positive strain.

The phytosomes are successfully developed *via* the thin film hydration method. The hydrophilic head of soy lecithin is oriented toward the external and core aqueous medium, and the hydrophobic tail remains away from the water. This arrangement facilitates the formation of a lipid bilayer vesicle.[46,47] The yield of each batch exceeding 94% indicates the suitability of the thin-film hydration method employed for the formulation of phytosomes. The vesicles were found to be nanometric in size (Z_{avg}: 71.03 ± 0.44 nm to 81.33 ± 1.11 nm) with a homogeneous nature (PDI < 0.5).[48] The ZP of all the formulations was within -38.83 ± 0.23 to -50.36 ± 0.43 mV, and the values greater than ± 30 mV represent high colloidal stability.[49]

The EE was found to be within 44.44 ± 1.23 to 60.71 ± 0.47 %, and the DL was found to be 6.93 ± 0.33 to 9.55 ± 0.27%. Based on the high percentage of EE, low PDI, high ZP values, and excellent stability, the P3 was selected as an optimized formula and used for further studies. The phytosome vesicles are found to be spherical in shape, with uniform size, having an average diameter of 20.329 ± 1.821nm (Figure 1b). The size of the vesicles was found to be slightly lower than the hydrodynamic vesicle size obtained by the DLS, which may be due to the shrinkage of the vesicles during the drying of the phytosome on the HR-TEM grid.

Better consistency with the homogeneity of gels is essential for patient compliance.[50,51] Carbopol based-gelling agent is selected due to its inert nature, outstanding bioadhesive characteristics, hydrophilic, non-irritating, non-toxic nature, compatibility with many active ingredients, and excellent thermal and storage stability.[52] Further, the carbopol-based gel can be formulated in water at ambient temperatures, whereas hydroxypropyl methylcellulose needs to be dissolved in hot water. Carbopol 934 is a synthetic, hydrophilic polymer widely exploited for the preparation of hydrogels for topical drug delivery. Due to excellent pharmaceutical properties, non-toxic nature, prolonged drug release, skin compatibility, wide range of pH compatibility, pseudoplastic behaviour, and remarkable storage stability, the carbopol 934 was selected for the development of phytosomal gel.[53,54]

The gel formulations are white in color and have a pleasant appearance. In contrast, G-SMf gel appears slightly yellowish in color, opaque, and homogeneous. The pH of phytosome-loaded gel was found to be within 5.49 ± 0.03 to 5.51 ± 0.06, which is close to the skin pH (5-6), reflecting the suitability of these gels for the topical application. Also, the pH of the gels is close to that of the marketed gel. Spreadability is one of the essential elements of a gel formulation related to user compliance. Patients have less discomfort when gels with appropriate spreadability are applied to the skin.[55] In this study, lower concentration G-0.5 gel shows higher spreadability (7.31 ± 0.06 cm). In contrast, higher concentration gel G-1.5 shows lower spreadability, 5.9 ± 0.053 cm, due to the gel's capacity to spread is influenced by polymer concentration, polymeric chain length, and polydispersity.[56] The G-1.0 showed the spreadability of 6.76 ± 0.10 cm, similar to the standard formulation of 6.63 ± 0.07 cm. The extrudability was found to be in the range of 113.28 ± 1.52 g to 182.23 ± 1.0 g, and G-1.0 gel (139.76 ± 2.22 g) was similar to the marketed gel (132.21 ± 2.10 g). The viscosity gradually increased with the gel concentration. The viscosity study results of G-1.0 gel (74333 ± 333.72 cP) are found to be similar to the marketed gel (73666 ± 333.72 cP). The gel slightly contracts during syneresis, and a small quantity of unbound water is squeezed out. It is an undesirable attribute that can be avoided by choosing the right gellant concentration.[57] With an increase in the carbopol 934 concentration, the syneresis was reduced, and G-1.0 showed a percentage of syneresis value (1.45 ± 0.15%)

comparable with the marketed gel (1.22 ± 0.10%), and the drug content value was shown to be > 96%.

The vibrational spectral analysis of the SL revealed a broad peak at 3271 cm^{-1}, indicating the stretching vibration of the phenolic -OH group. The peaks at 2914 cm^{-1} and 2842 cm^{-1} are attributed to the C-H stretching of alkanes. Further vibrational bands at 1732 cm^{-1} and 1466 cm^{-1} correspond to the stretching of carbonyl C = O and the bending of C-H in alkanes, respectively. Additionally, the peak observed at 1226 cm^{-1} is due to the stretching vibration of P = O.[46,58,59] CHL exhibits distinctive peaks in its infrared spectrum. At 3383 cm^{-1}, a broad peak arises from the O-H vibration. The sharper peaks at 2922 cm^{-1} and 2849 cm^{-1} are attributed to the asymmetric stretching vibrations of C-H bonds within methyl groups. A distinct peak at 1466 cm^{-1} indicates either the stretching of the C = C bond or the bending of the C-H bond. Peaks at 1368 cm^{-1} and 1230 cm^{-1} correspond to C-O stretching in the C-O-H group and O-H bending, respectively. Additional features include a vibrational band at 1044 cm-1 associated with stretching of the C-O bond. Peaks at 947 cm^{-1} and 834 cm^{-1} are assigned to the C-C backbone vibration. Lastly, the peak at 793 cm^{-1} is due to the C–H out-of-plane vibrations, as documented by Paradkar et al.[60] The physical mixture showed the superimposed peaks of SMf, SL, and CHL. The characteristic peaks of SMf (2922, 2860, 1715, 1448, 1372, 1229, and 1160 cm^{-1}) are found to be retained in the PM, representing the retention of chemical property compatibility with the excipients. In C-934, a very broad peak around 3011 cm^{-1} is due to the stretching of the -OH group. A sharp characteristic band at about 1708 cm^{-1} due to C = O stretching: weak peaks at 1417-1449 cm^{-1} are ascribed to the stretching of the C-O group. The band at 1239 cm^{-1} is assigned to the vibration of C-O-C of acrylates. The bands at 1174 cm^{-1} and 802 cm^{-1} are ascribed to the ethereal cross-linking and out-of-plane bending of = C–H groups, respectively.[61] The TEA showed a broad peak from 2100-3000 cm^{-1}, corresponding to -OH stretching. The peaks at 1900 cm^{-1}, 1756 cm^{-1}, and 1634 cm^{-1} are ascribed to the stretching of the -CH_2-group.

The peak at 3414 cm^{-1} in the phytosome gel corresponds to the spectral overlap for SMf, SL, and CHL due to OH stretching. This overlap, characterized by a broad and intense band, is well established as the fingerprint region. The distinctive strong peaks at 2923 cm^{-1} and 2846 cm^{-1} result from CH_2 symmetric stretching. The prominent band at 1728 cm^{-1} is attributed to the carbonyl C = O stretching vibration of C-934. The phytosome gel exhibits all the characteristic peaks of SMf (2923, 2858, 1719, 1539, 1452, 1374, and 1230 cm^{-1}), although with reduced intensity and no shifting. This indicates that the chemical integrity and compatibility between the drug and excipients are maintained. The decrease in intensity can be attributed to the dilution effect caused by the excipients.

Goat and cow skin have been extensively used in ex vivo skin permeability studies. Both cow and goat hides possess epidermal and dermal layers that exhibit distinct characteristics similar to human skin. In contrast, the skin of laboratory animals such as rabbits, mice, guinea pigs, and rats shows significant anatomical differences compared to human skin. These animals have a notably thin epidermis and a flat epidermal-dermal interface that lacks ridges and papillary projections. Obtaining ethical approval for research involving human skin and primates can be challenging.[62] Therefore, we selected the goat skin in ex vivo permeation studies of SMf-loaded plain gel and phytosome gel with the help of the Franz diffusion cell. Phytosomes signify a breakthrough in the administration of herbal remedies, improving the bioavailability and stability of phytochemical components. The unique characteristics of phytosomes, such as safeguarding active compounds from deterioration, improving skin absorption, and facilitating precise drug delivery, have positioned them as a potential nanocarrier system in the pharmaceutical, cosmeceutical, and nutraceutical sectors.[20] Unlike a raw herbal extract, its nanovesicles demonstrated increased flux and better drug retention within the skin layers. Topical nano gels facilitate drug delivery by retaining and hydrating the drug within the skin.[63] Due to their nanostructure, they easily permeate through the skin barriers. Further, the lipid-based structure of phytosomes allows them to interact with the skin's lipid-rich layers due to their high affinity, facilitating penetration and absorption. Additionally, the phytosomes form hydrogen bonds with the phytoconstituents, improving their stability and skin penetration compared to free phytoconstituents. Moreover, phytosomes also improve skin functions by improving hydration, enzyme balance, and collagen structure.[64] In a recent study, olive oil containing phytosomal nanocarriers of quercetin was reported for improved skin permeability. The phytosomal nanocarriers were prepared by a solvent evaporation/anti-solvent precipitation technique and optimized using a Box-Behnken design. The formulation showed significantly higher skin permeation of quercetin compared to an olive-oil/surfactant-free formulation and the control.[22] In another study, a phytosomal gel of aloe vera extract was studied for topical drug delivery. A 2^2 Factorial design was used to develop and statistically optimize the formulation with respect to vesicular size and entrapment efficiency. The optimized phytosome was loaded into carbopol 934 to develop a phytosomal gel. The phytosomal gel showed a significantly higher permeation and flux profile than the conventional aloe vera extract gel.[8] In a recent study, a phytosomal gel of *Cassia alata* leaf extract was prepared and evaluated for its antibacterial activity against *Staphylococcus aureus* and *Escherichia coli*. The developed phytosomal gel demonstrated excellent pharmaceutical properties, pH, spreadability, and extrudability. The nanovesicular gel showed improved antibacterial activity compared to the neat extract and plain gel.[65] Our study demonstrated that phytosome gel (G-1.0) displayed excellent pharmaceutical outcomes with significantly

improved ex-vivo skin permeability steady-state flux (Jss), permeability coefficient (Kp), and enhancement ratio (Er) compared to extract-loaded plain gel. Singh et al[66] study results of ex-vivo skin permeability steady-state flux from *Hedyotis corymbosa* (L.) Lam. extract and evaluated for its efficacy in psoriasis. The optimized phytosome was incorporated in a pluronic gel for the development of phytosomal gel. The extract-loaded pluronic gel showed a flux of only 2.78μg/cm^2/h compared to the optimised Phytosomal Pluronic gel with a flux value of 5.24μg/cm^2/h. The phytosomal gel demonstrated improved dermatokinetics compared to the extract-loaded pluronic gel. The phytosomal nanogel improved skin integrity and downregulated inflammatory cytokines with improved anti-psoriatic activity compared to the marketed product. At the end of ex-vivo skin permeability studies with extract-loaded plain gel (G-plain) and phytosome gel (G-1.0) with the help of vertical Franz diffusion, no apparent damage (signs of tears, cuts, imperfections, and cracking) on the goat skin was observed. Further, the maintenance of skin thickness and skin hydration level before and after the diffusion study supports the retention of membrane integrity. The presence of sodium azide (0.0025% w/v) in the medium avoids possible microbial deterioration of the membrane and growth in the media.

The stability test was performed with the optimized formulation of SMf-loaded phytosome P3 (1:3:0.25 ratio of SMf, soya lecithin, and cholesterol). The phytosome demonstrated aggregation, fusion, and the potential disruption of vesicles throughout the conducted three heating–cooling cycles stability test. The instability observed in phytosome formulations can be identified by an increase in the size of up to 204 nm of the vesicles resulting from alterations at the end of the heating–cooling cycles. A higher PDI signifies a lower uniformity in the preparation.[67] The heating–cooling cycles of the optimized formulation of SMf-loaded 1.0 % w/v phytosome gel through physical appearance after three cycles show slight smoothness, slight color change, and no visible aggregation during the cycles. Syneresis is a frequently encountered issue related to the physical stability of gel formulation. It occurs when the dispersion medium is expelled due to the elastic contraction of the polymeric gelling agents. The liquid loss of phytosome gel up to 3.32% at the end indicates the gelling agent can contract, squeezing out the water. Meanwhile, the overall cycle maintains the stability of the products.[68]

The extract exhibits very mild signs of skin dryness and irritation. However, G-1.0 showed a primary irritation index of zero, representing its non-irritating nature, comparable to the untreated control. The non-irritancy of G-1.0 is due to the entrapment of SMf in the phytosome nanovesicle of the phytosome gel, which avoids the direct contact of SMf with the skin.

The DNCB-induced AD model is widely exploited as an AD model in BALB/c mice.[69-73]Human-like AD in pre-clinical models can be induced by using mice with spontaneously developing skin eczema, genetically modified mice, or chemical sensitization. Among them, the chemical sensitization method is the most common. The 2,4-dinitrochlorobenzene (DNCB) is a standard compound for inducing contact sensitization and the formation of multiple haptens with extracellular and intracellular proteins in human skin. Repeated DNCB irritation of the murine skin is described in two phases: a sensitization phase (first contact with the hapten) and a challenging phase (second hapten encounter). It effectively mimics the key features of human AD, including skin inflammation, immune dysregulation, and altered skin barrier function, relatively easy to establish, making it a valuable model for research. BALB/c mice are a commonly used model due to their susceptibility to allergic reactions and DNCB sensitization.[74-77]

The blood cells, *viz.* white blood cells (WBCs), monocytes, lymphocytes, neutrophils, and eosinophils, are necessary for defence against pathogenic organisms. Compared to the healthy control, in the case of AD, there is a considerably increased amount of WBC, neutrophils, lymphocytes, and eosinophils.[78,79] We analyzed the leukocyte counts in cardiovascular blood samples employing a Neubauer hemocytometer to determine whether cutaneous G-1.0 sensitization may reduce the inflammatory cells. The study demonstrates that G-1.0 dramatically reduced the levels of lymphocytes, monocytes, eosinophils, and neutrophils, comparable to the standard marketed drug. Additionally, G-1.0 outperformed other formulations in effectiveness, such as G-plain, G-placebo, SMf, and G-SMf.

The DNCB-treated group had much thicker ears and spleen weights than the normal control group due to the repeated topical application of DNCB. The phytosome gel G-1.0 group exhibited decreased ear thickness and spleen weight throughout the trial period. AD can impact the immune system because it frequently manifests as a systemic immunological response. We examined the ear thickness and spleen weight on the last day to determine if applying phytosome gel G-1.0 topically to mice had an anti-AD effect. The disease control group's results revealed increased spleen weight and ear thickness compared to the control group (normal), while the G-1.0 therapy group displayed inhibition. These findings thus indicate that topical G-1.0 treatment may have an anti-AD effect.[39,40] Previous studies[80] showed that β-sitosterol decreased IgE levels and blood histamine in the DNCB-induced AD model and histamine-induced scratching behaviours in mice. It also reduced clinical signs of AD, such as erythema, dryness, and eczema. Furthermore, β-sitosterol reduced expression in skin lesions resembling AD. These results suggest that β-sitosterol may have therapeutic value for AD and other skin inflammations.

The health benefits and biological properties of the flowering buds of *Mesua ferrea* Linn. have been studied intensively over the past three decades in terms of various activities, *viz.* antimicrobial, anti-allergic effects, anti-

inflammatory, and antioxidant activity. [9,10] The curative effects of G-1.0 on skin disease and its complications are related to its inhibition of cell response. The primary finding of this research work is that G-1.0 modulates the reduction of activation in TNF-α-induced cells and decreases the formation of DNCB-induced AD lesions in BALB/c mice.[40] The data gathered from the research will be used for preclinical trials, clinical research, and the pilot plant scale-up techniques, which will improve its translational value. This optimal utilization of benefits and costs will aid in technology transfer, and the product's translational value will also hold commercial significance.

Conclusion

The n-hexane extract of *Mesua ferrea* Linn. has shown potential anti-microbial effects against *S. aureus*. Further, the presence of β-sitosterol supports its use for treating AD diseases. The current research focused on developing a pharmaceutically standardized phytosome formulation loaded with SMf, utilizing assessment techniques including achieving nano-size particles, optimizing drug loading capacity, attaining high encapsulation efficiency, high zeta potential, and low PDI. The formulated SMf-loaded phytosome was subsequently integrated into a gel formulation. The gel formulation was characterized for organoleptic properties, drug content, syneresis, extrudability, spreadability, viscosity, homogeneity, pH, ATR-FTIR study for drug-excipient compatibility, permeability study, stability study, and in-vivo activity against AD in DNCB-induced BALB/c female mice. The G-1.0 formulation showed improved pharmaceutical properties and efficient skin permeability compared to standardized extract-loaded plain gel with a non-irritating nature. The results of the AD study in the DNCB mice model showed improved therapeutic potential of SMf-loaded phytosome gel (G-1.0) compared to SMf-loaded plain gel. These effects of SMf with a novel topical drug delivery system can be a latent alternative treatment for AD. However, a detailed clinical evaluation is necessary to understand the exact pharmacokinetic and pharmacodynamic fate of the standardized herbal extract in a novel phytosome gel for an effective AD treatment.

Acknowledgements

The author wishes to express gratitude to Ganesh Dey, Simran Giri, and Ramesh for their invaluable assistance and support throughout the research. In addition, the authors would like to acknowledge the Department of Pharmaceutical Engineering & Technology at IIT (BHU), Shree Harish Chandra PG College and the University of North Bengal for providing the facility and continuous support.

Authors' Contribution

Conceptualization: Alakh Niranjan Sahu, Debadatta Mohapatra, Bapi Ray Sarkar.
Data curation: Debadatta Mohapatra, Jugal Sutradhar, Nirupam Das.
Formal analysis: Nirupam Das, Debadatta Mohapatra, Jugal Sutradhar, Bapi Ray Sarkar, Alakh Niranjan Sahu.
Investigation: Alakh Niranjan Sahu, Nirupam Das, Debadatta Mohapatra.
Methodology: Debadatta Mohapatra, Jugal Sutradhar.
Project administration: Bapi Ray Sarkar, Alakh Niranjan Sahu, Nirupam Das, Debadatta Mohapatra.
Software: Debadatta Mohapatra, Jugal Sutradhar.
Supervision: Bapi Ray Sarkar, Alakh Niranjan Sahu, Debadatta Mohapatra, Nirupam Das.
Validation: Nirupam Das, Bapi Ray Sarkar**,** Debadatta Mohapatra, Alakh Niranjan Sahu.
Visualization: Jugal Sutradhar, Nirupam Das, Debadatta Mohapatra.
Writing-original draft: Jugal Sutradhar.
Writing-review & editing: Debadatta Mohapatra, Nirupam Das, Bapi Ray Sarkar, Alakh Niranjan Sahu.

Competing Interests

All authors declare no conflict of interest.

Ethical Approval

The necessary approval was obtained from Deshpande Laboratories Pvt. Ltd. for conducting the animal studies with number 1582/PO/Re/S/11/ CPCSEA, Date. 31.01.2023 and by the recommendations of the CPCSEA.

Funding

This research study received no financial support.

Informed Consent

Not required.

References

1. Lin CY, Hsieh YT, Chan LY, Yang TY, Maeda T, Chang TM, et al. Dictamnine delivered by PLGA nanocarriers ameliorated inflammation in an oxazolone-induced dermatitis mouse model. J Control Release. 2021;329:731-42. doi: 10.1016/j.jconrel.2020.10.007.
2. Langan SM, Irvine AD, Weidinger S. Atopic dermatitis. Lancet. 2020;396(10247):345-60. doi: 10.1016/s0140-6736(20)31286-1.
3. Birdi G, Cooke R, Knibb RC. Impact of atopic dermatitis on quality of life in adults: a systematic review and meta-analysis. Int J Dermatol. 2020;59(4):e75-91. doi: 10.1111/ijd.14763.
4. GBD 2021 Asthma and Allergic Diseases Collaborators. Global, regional, and national burden of asthma and atopic dermatitis, 1990-2021, and projections to 2050: a systematic analysis of the Global Burden of Disease Study 2021. Lancet Respir Med. 2025;13(5):425-46. doi: 10.1016/s2213-2600(25)00003-7.
5. Kim J, Kim BE, Leung DY. Pathophysiology of atopic dermatitis: clinical implications. Allergy Asthma Proc. 2019;40(2):84-92. doi: 10.2500/aap.2019.40.4202.
6. Ramos Campos EV, De Freitas Proença PL, Doretto-Silva L, Andrade-Oliveira V, Fraceto LF, de Araujo DR. Trends in nanoformulations for atopic dermatitis treatment. Expert Opin Drug Deliv. 2020;17(11):1615-30. doi: 10.1080/17425247.2020.1813107.
7. Harvey J, Lax SJ, Lowe A, Santer M, Lawton S, Langan SM, et al. The long-term safety of topical corticosteroids in atopic dermatitis: a systematic review. Skin Health Dis. 2023;3(5):e268. doi: 10.1002/ski2.268.
8. Jain P, Taleuzzaman M, Kala C, Kumar Gupta D, Ali A, Aslam M. Quality by design (Qbd) assisted development of phytosomal gel of *Aloe vera* extract for topical delivery. J Liposome Res. 2021;31(4):381-8. doi: 10.1080/08982104.2020.1849279.
9. Rajalakshmi P, Vadivel V, Ravichandran N, Brindha P. Investigation on pharmacognostic parameters of sirunagapoo (*Mesua ferrea* L): a traditional Indian herbal drug. Pharmacogn J. 2019;11(2):225-30. doi: 10.5530/pj.2019.11.35.
10. Wang S, Guo Y, Yao D, Liu L, Duan H, Meng L, et al. 4-Alkyl-5,7-dihydroxycoumarins from the flowering buds of

Mesua ferrea. Fitoterapia. 2019;138:104192. doi: 10.1016/j.fitote.2019.104192.
11. Nagalingam A. Drug delivery aspects of herbal medicines. In: Arumugam S, Watanabe K, eds. Japanese Kampo Medicines for the Treatment of Common Diseases: Focus on Inflammation. Academic Press; 2017. p. 143-64. doi: 10.1016/b978-0-12-809398-6.00015-9.
12. Ajazuddin, Saraf S. Applications of novel drug delivery system for herbal formulations. Fitoterapia. 2010;81(7):680-9. doi: 10.1016/j.fitote.2010.05.001.
13. Lu M, Qiu Q, Luo X, Liu X, Sun J, Wang C, et al. Phyto-phospholipid complexes (phytosomes): a novel strategy to improve the bioavailability of active constituents. Asian J Pharm Sci. 2019;14(3):265-74. doi: 10.1016/j.ajps.2018.05.011.
14. Barani M, Sangiovanni E, Angarano M, Rajizadeh MA, Mehrabani M, Piazza S, et al. Phytosomes as innovative delivery systems for phytochemicals: a comprehensive review of literature. Int J Nanomedicine. 2021;16:6983-7022. doi: 10.2147/ijn.S318416.
15. Gaikwad SS, Morade YY, Kothule AM, Kshirsagar SJ, Laddha UD, Salunkhe KS. Overview of phytosomes in treating cancer: advancement, challenges, and future outlook. Heliyon. 2023;9(6):e16561. doi: 10.1016/j.heliyon.2023.e16561.
16. Witika BA, Mweetwa LL, Tshiamo KO, Edler K, Matafwali SK, Ntemi PV, et al. Vesicular drug delivery for the treatment of topical disorders: current and future perspectives. J Pharm Pharmacol. 2021;73(11):1427-41. doi: 10.1093/jpp/rgab082.
17. Sahu AN, Mohapatra D. Nanovesicular transferosomes for the topical delivery of plant bioactives. Nanomedicine (Lond). 2021;16(28):2491-5. doi: 10.2217/nnm-2021-0316.
18. Khogta S, Patel J, Barve K, Londhe V. Herbal nano-formulations for topical delivery. J Herb Med. 2020;20:100300. doi: 10.1016/j.hermed.2019.100300.
19. Mirzaei H, Shakeri A, Rashidi B, Jalili A, Banikazemi Z, Sahebkar A. Phytosomal curcumin: a review of pharmacokinetic, experimental and clinical studies. Biomed Pharmacother. 2017;85:102-12. doi: 10.1016/j.biopha.2016.11.098.
20. Talebi M, Shahbazi K, Dakkali MS, Akbari M, Almasi Ghale R, Hashemi S, et al. Phytosomes: a promising nanocarrier system for enhanced bioavailability and therapeutic efficacy of herbal products. Phytomed Plus. 2025;5(2):100779. doi: 10.1016/j.phyplu.2025.100779.
21. Vishwakarma DK, Mishra JN, Shukla AK, Singh AP. Phytosomes as a novel approach to drug delivery system. In: Afrin F, Bhuniya S, eds. Smart Drug Delivery Systems-Futuristic Window in Cancer Therapy. IntechOpen; 2024. doi: 10.5772/intechopen.113914.
22. Hendawy OM, Al-Sanea MM, Elbargisy RM, Rahman HU, Gomaa HA, Mohamed AA, et al. Development of olive oil containing phytosomal nanocomplex for improving skin delivery of quercetin: formulation design optimization, in vitro and ex vivo appraisals. Pharmaceutics. 2023;15(4):1124. doi: 10.3390/pharmaceutics15041124.
23. Sutradhar J, Sarkar BR. Qualitative assessment of the flowering buds of *Mesua ferrea* Linn with special emphasize on HPTLC and universal DNA bar-coding technique and evaluation of its antimicrobial potential. Futur J Pharm Sci. 2024;10(1):21. doi: 10.1186/s43094-024-00596-3.
24. Sutradhar J, Sarkar BR. Quantification of β-sitosterol by validated high performance thin layer chromatography (HPTLC) densitometric method in the flowering buds of *Mesua ferrea* Linn. J Sci Res. 2023;15(3):879-86. doi: 10.3329/jsr.v15i3.64274.
25. Nagaich U, Gulati N. Nanostructured lipid carriers (NLC) based controlled release topical gel of clobetasol propionate: design and in vivo characterization. Drug Deliv Transl Res. 2016;6(3):289-98. doi: 10.1007/s13346-016-0291-1.
26. Khan AW, Kotta S, Ansari SH, Sharma RK, Kumar A, Ali J. Formulation development, optimization and evaluation of *Aloe vera* gel for wound healing. Pharmacogn Mag. 2013;9(Suppl 1):S6-10. doi: 10.4103/0973-1296.117849.
27. Bachhav YG, Patravale VB. Microemulsion based vaginal gel of fluconazole: formulation, in vitro and in vivo evaluation. Int J Pharm. 2009;365(1-2):175-9. doi: 10.1016/j.ijpharm.2008.08.021.
28. Banerjee S, Bhattacharya S. Compressive textural attributes, opacity and syneresis of gels prepared from gellan, agar and their mixtures. J Food Eng. 2011;102(3):287-92. doi: 10.1016/j.jfoodeng.2010.08.025.
29. Shukla R, Tiwari G, Tiwari R, Rai AK. Formulation and evaluation of the topical ethosomal gel of melatonin to prevent UV radiation. J Cosmet Dermatol. 2020;19(8):2093-104. doi: 10.1111/jocd.13251.
30. Das B, Sen SO, Maji R, Nayak AK, Sen KK. Transferosomal gel for transdermal delivery of risperidone: formulation optimization and ex vivo permeation. J Drug Deliv Sci Technol. 2017;38:59-71. doi: 10.1016/j.jddst.2017.01.006.
31. Habib BA, Sayed S, Elsayed GM. Enhanced transdermal delivery of ondansetron using nanovesicular systems: fabrication, characterization, optimization and ex-vivo permeation study-Box-Cox transformation practical example. Eur J Pharm Sci. 2018;115:352-61. doi: 10.1016/j.ejps.2018.01.044.
32. González-Rodríguez ML, Arroyo CM, Cózar-Bernal MJ, González RP, León JM, Calle M, et al. Deformability properties of timolol-loaded transfersomes based on the extrusion mechanism. Statistical optimization of the process. Drug Dev Ind Pharm. 2016;42(10):1683-94. doi: 10.3109/03639045.2016.1165691.
33. Elkomy MH, El Menshawe SF, Abou-Taleb HA, Elkarmalawy MH. Loratadine bioavailability via buccal transferosomal gel: formulation, statistical optimization, in vitro/in vivo characterization, and pharmacokinetics in human volunteers. Drug Deliv. 2017;24(1):781-91. doi: 10.1080/10717544.2017.1321061.
34. Tunit P, Thammarat P, Okonogi S, Chittasupho C. Hydrogel containing *Borassus flabellifer* L. male flower extract for antioxidant, antimicrobial, and anti-inflammatory activity. Gels. 2022;8(2):126. doi: 10.3390/gels8020126.
35. Percie du Sert N, Ahluwalia A, Alam S, Avey MT, Baker M, Browne WJ, et al. Reporting animal research: explanation and elaboration for the ARRIVE guidelines 2.0. PLoS Biol. 2020;18(7):e3000411. doi: 10.1371/journal.pbio.3000411
36. OECD. Test No. 402: Acute Dermal Toxicity. Paris: OECD Publishing; 2017. doi: 10.1787/9789264070585-en.
37. Djerrou Z, Djaalab H, Riachi F, Serakta M, Chettoum A, Maameri Z, et al. Irritantcy potential and sub-acute dermal toxicity study of *Pistacia lentiscus* fatty oil as a topical traditional remedy. Afr J Tradit Complement Altern Med. 2013;10(3):480-9. doi: 10.4314/ajtcam.v10i3.15.
38. Wang Y, Zhang P, Zhang J, Hong T. Inhibitory effect of bisdemethoxycurcumin on DNCB-induced atopic dermatitis in mice. Molecules. 2022;28(1):293. doi: 10.3390/molecules28010293.
39. Park SH, Jang S, An JE, Choo BK, Kim HK. *I. inflexus* (Thunb.) Kudo extract improves atopic dermatitis and depressive-like behavior in DfE-induced atopic dermatitis-like disease. Phytomedicine. 2020;67:153137. doi: 10.1016/j.phymed.2019.153137.
40. Yang HR, Lee H, Kim JH, Hong IH, Hwang DH, Rho IR, et al. Therapeutic effect of *Rumex japonicus* Houtt. on DNCB-induced atopic dermatitis-like skin lesions in BALB/c mice and human keratinocyte HaCaT cells. Nutrients. 2019;11(3):573. doi: 10.3390/nu11030573 .
41. Gil TY, Kang YM, Eom YJ, Hong CH, An HJ. Anti-atopic dermatitis effect of seaweed fulvescens extract via inhibiting the STAT1 pathway. Mediators Inflamm. 2019;2019:3760934.

doi: 10.1155/2019/3760934.
42. Brandt EB, Sivaprasad U. Th2 cytokines and atopic dermatitis. J Clin Cell Immunol. 2011;2(3):110. doi: 10.4172/2155-9899.1000110.
43. ICH Harmonised Tripartite Guideline. Validation of Analytical Procedures: Text and Methodology, Q2(R1). ICH; 2005. Available from: https://database.ich.org/sites/default/files/Q2%28R1%29%20Guideline.pdf. Published November 11, 2023. Accessed January 8, 2025.
44. Bath-Hextall FJ, Birnie AJ, Ravenscroft JC, Williams HC. Interventions to reduce *Staphylococcus aureus* in the management of atopic eczema: an updated Cochrane review. Br J Dermatol. 2010;163(1):12-26. doi: 10.1111/j.1365-2133.2010.09743.x.
45. Torres T, Ferreira EO, Gonçalo M, Mendes-Bastos P, Selores M, Filipe P. Update on atopic dermatitis. Acta Med Port. 2019;32(9):606-13. doi: 10.20344/amp.11963.
46. Singh RP, Gangadharappa HV, Mruthunjaya K. Phytosome complexed with chitosan for gingerol delivery in the treatment of respiratory infection: in vitro and in vivo evaluation. Eur J Pharm Sci. 2018;122:214-29. doi: 10.1016/j.ejps.2018.06.028.
47. Mahapatra DK, Patil S, Patil AG. The progressive journey of phytosomes in herbal based pharmacotherapeutics. Curr Bioact Compd. 2020;16(6):853-86. doi: 10.2174/1573407215666190417121237.
48. Wanjiru J, Gathirwa J, Sauli E, Swai HS. Formulation, optimization, and evaluation of *Moringa oleifera* leaf polyphenol-loaded phytosome delivery system against breast cancer cell lines. Molecules. 2022;27(14):4430. doi: 10.3390/molecules27144430.
49. Mohapatra D, Alam MB, Pandey V, Pratap R, Dubey PK, Parmar AS, et al. Carbon dots from an immunomodulatory plant for cancer cell imaging, free radical scavenging and metal sensing applications. Nanomedicine (Lond). 2021;16(23):2039-59. doi: 10.2217/nnm-2021-0190.
50. Ahad A, Al-Saleh AA, Al-Mohizea AM, Al-Jenoobi FI, Raish M, Yassin AEB, et al. Pharmacodynamic study of eprosartan mesylate-loaded transfersomes Carbopol® gel under Dermaroller® on rats with methyl prednisolone acetate-induced hypertension. Biomed Pharmacother. 2017;89:177-84. doi: 10.1016/j.biopha.2017.01.164.
51. Vasanth S, Dubey A, Ravi GS, Lewis SA, Ghate VM, El-Zahaby SA, et al. Development and investigation of vitamin C-enriched adapalene-loaded transfersome gel: a collegial approach for the treatment of *Acne vulgaris*. AAPS PharmSciTech. 2020;21(2):61. doi: 10.1208/s12249-019-1518-5.
52. Tafish AM, El-Sherbiny M, Al-Karmalawy AA, Soliman OA, Saleh NM. Carvacrol-loaded phytosomes for enhanced wound healing: molecular docking, formulation, DoE-aided optimization, and in vitro/in vivo evaluation. Int J Nanomedicine. 2023;18:5749-80. doi: 10.2147/ijn.S421617.
53. Lee SG, Kang JB, Kim SR, Kim CJ, Yeom DW, Yoon HY, et al. Enhanced topical delivery of tacrolimus by a carbomer hydrogel formulation with transcutol P. Drug Dev Ind Pharm. 2016;42(10):1636-42. doi: 10.3109/03639045.2016.1160107.
54. Hamdi NA, Azmi NA, Sabari NH, Harun AF, Haris MS. An insight into the use and advantages of Carbopol in topical mucoadhesive drug delivery system: a systematic review. J Pharm. 2023;3(1):53-65. doi: 10.31436/jop.v3i1.156.
55. Permana AD, Utami RN, Courtenay AJ, Manggau MA, Donnelly RF, Rahman L. Phytosomal nanocarriers as platforms for improved delivery of natural antioxidant and photoprotective compounds in propolis: an approach for enhanced both dissolution behaviour in biorelevant media and skin retention profiles. J Photochem Photobiol B. 2020;205:111846. doi: 10.1016/j.jphotobiol.2020.111846.
56. Ontong JC, Singh S, Nwabor OF, Chusri S, Voravuthikunchai SP. Potential of antimicrobial topical gel with synthesized biogenic silver nanoparticle using *Rhodomyrtus tomentosa* leaf extract and silk sericin. Biotechnol Lett. 2020;42(12):2653-64. doi: 10.1007/s10529-020-02971-5.
57. Dixit KO, Mohapatra DE, Senapati PC, Panda R, Sahu AN. Formulation development and evaluation of *Lawsonia inermis* extract loaded hydrogel for wound dressing application. Indian J Pharm Sci. 2022;84(4):848-62. doi: 10.36468/pharmaceutical-sciences.980.
58. Singh VK, Pandey PM, Agarwal T, Kumar D, Banerjee I, Anis A, et al. Development of soy lecithin based novel self-assembled emulsion hydrogels. J Mech Behav Biomed Mater. 2015;55:250-63. doi: 10.1016/j.jmbbm.2015.10.027.
59. Hou Z, Li Y, Huang Y, Zhou C, Lin J, Wang Y, et al. Phytosomes loaded with mitomycin C-soybean phosphatidylcholine complex developed for drug delivery. Mol Pharm. 2013;10(1):90-101. doi: 10.1021/mp300489p.
60. Paradkar MM, Irudayaraj J. Determination of cholesterol in dairy products using infrared techniques: 1. FTIR spectroscopy. Int J Dairy Technol. 2002;55(3):127-32. doi: 10.1046/j.1471-0307.2002.00044.x.
61. Sahoo S, Chakraborti CK, Behera PK, Mishra SC. FTIR and Raman spectroscopic investigations of a norfloxacin/Carbopol934 polymerie suspension. J Young Pharm. 2012;4(3):138-45. doi: 10.4103/0975-1483.100017.
62. Ahmad N, Ahmad R, Mohammed Buheazaha T, Salman AlHomoud H, Al-Nasif HA, Sarafroz M. A comparative ex vivo permeation evaluation of a novel 5-fluorocuracil nanoemulsion-gel by topically applied in the different excised rat, goat, and cow skin. Saudi J Biol Sci. 2020;27(4):1024-40. doi: 10.1016/j.sjbs.2020.02.014.
63. Raina N, Rani R, Thakur VK, Gupta M. New insights in topical drug delivery for skin disorders: from a nanotechnological perspective. ACS Omega. 2023;8(22):19145-67. doi: 10.1021/acsomega.2c08016.
64. Alharbi WS, Almughem FA, Almehmady AM, Jarallah SJ, Alsharif WK, Alzahrani NM, et al. Phytosomes as an emerging nanotechnology platform for the topical delivery of bioactive phytochemicals. Pharmaceutics. 2021;13(9):1475. doi: 10.3390/pharmaceutics13091475.
65. Alalor CA, Okafo SE, Agbamu E, Ayewunmi E. Evaluation of the antibacterial potentials of phytosomal gel of *Cassia alata* leaf extract. Dutse J Pure Appl Sci. 2024;10(3b):53-61. doi: 10.4314/dujopas.v10i3b.7.
66. Singh N, Shaikh AM, Gupta P, Kovács B, Abuzinadah MF, Ahmad A, et al. Nanophytosomal gel of *Heydotis corymbosa* (L.) extract against psoriasis: characterisation, in vitro and in vivo biological activity. Pharmaceuticals (Basel). 2024;17(2):213. doi: 10.3390/ph17020213.
67. Maryana W, Rachmawati H, Mudhakir D. Formation of phytosome containing silymarin using thin layer-hydration technique aimed for oral delivery. Mater Today Proc. 2016;3(3):855-66. doi: 10.1016/j.matpr.2016.02.019.
68. Guo H, Ge J, Wu Q, He Z, Wang W, Cao G. Syneresis behavior of polymer gels aged in different brines from gelants. Gels. 2022;8(3):166. doi: 10.3390/gels8030166.
69. Lee Y, Choi HK, Ulrich N'deh KP, Choi YJ, Fan M, Kim EK, et al. Inhibitory effect of *Centella asiatica* extract on DNCB-induced atopic dermatitis in HaCaT cells and BALB/c mice. Nutrients. 2020;12(2):411. doi: 10.3390/nu12020411.
70. Min GY, Kim EY, Hong S, Kim JH, Kim M, Kim EJ, et al. *Lycopus lucidus* Turcz ameliorates DNCB-induced atopic dermatitis in BALB/c mice. Mol Med Rep. 2021;24(6):827. doi: 10.3892/mmr.2021.12467.
71. Zeng ZW, Huang JQ, Chen Y, Yu X, Zhu W, Zhang DS. Acupoint autohemotherapy attenuates atopic dermatitis lesions by regulating Th1/Th2 balance in DNCB-induced

BALB/c mice. Chin J Integr Med. 2022;28(7):612-9. doi: 10.1007/s11655-022-3579-7.
72. Wang L, Xian YF, Loo SKF, Ip SP, Yang W, Chan WY, et al. Baicalin ameliorates 2,4-dinitrochlorobenzene-induced atopic dermatitis-like skin lesions in mice through modulating skin barrier function, gut microbiota and JAK/STAT pathway. Bioorg Chem. 2022;119:105538. doi: 10.1016/j.bioorg.2021.105538.
73. Yang CC, Hung YL, Ko WC, Tsai YJ, Chang JF, Liang CW, et al. Effect of neferine on DNCB-induced atopic dermatitis in HaCaT cells and BALB/c mice. Int J Mol Sci. 2021;22(15):8237. doi: 10.3390/ijms22158237.
74. Riedl R, Kühn A, Rietz D, Hebecker B, Glowalla KG, Peltner LK, et al. Establishment and characterization of mild atopic dermatitis in the DNCB-induced mouse model. Int J Mol Sci. 2023;24(15):12325. doi: 10.3390/ijms241512325.
75. Chattopadhyay R, Iswar S, Chakrabartti S, Mondal S, Modak P, Ghosh P, et al. Effect of L-theanine in the prevention of 2,4- dinitrochlorobenzene induced atopic dermatitis: a study in BALB/c mice model. Toxicol Rep. 2025;14:101984. doi: 10.1016/j.toxrep.2025.101984.
76. Ye S, Zhu L, Ruan T, Jia J, Mo X, Yan F, et al. Comparative study of mouse models of atopic dermatitis. Heliyon. 2025;11(2):e41989. doi: 10.1016/j.heliyon.2025.e41989.
77. Lee KS, Jeong ES, Heo SH, Seo JH, Jeong DG, Choi YK. A novel model for human atopic dermatitis: application of repeated DNCB patch in BALB/c mice, in comparison with NC/Nga mice. Lab Anim Res. 2010;26(1):95-102. doi: 10.5625/lar.2010.26.1.95.
78. Jiang Y, Ma W. Assessment of neutrophil-to-lymphocyte ratio and platelet-to-lymphocyte ratio in atopic dermatitis patients. Med Sci Monit. 2017;23:1340-6. doi: 10.12659/msm.900212.
79. Novak N, Allam P, Geiger E, Bieber T. Characterization of monocyte subtypes in the allergic form of atopic eczema/dermatitis syndrome. Allergy. 2002;57(10):931-5. doi: 10.1034/j.1398-9995.2002.23737.x.
80. Kim SJ. The ameliorative effect of β-sitosterol on DNCB-induced atopic dermatitis in mice. Biomed Sci Lett. 2017;23(4):303-9. doi: 10.15616/bsl.2017.23.4.303.